Erin C. Smith and Ian S. McLean, "Ground-based commissioning of FLITECAM", Proc. SPIE 7014, 701411 (2008).

http://dx.doi.org/10.1117/12.788693

Ground-based commissioning of FLITECAM

Erin C. Smith*[a] and Ian S. McLean[a]
[a]Dept. Physics and Astronomy, Univ. of California/Los Angeles, Los Angeles CA USA 90095-1562

ABSTRACT

FLITECAM is a 1-5 micron spectrometer and camera developed at UCLA for NASA's Stratospheric Observatory for Infrared Astronomy (SOFIA). On SOFIA, FLITECAM will take advantage of lower backgrounds from 3-5 microns and will provide access to spectral regions completely or partially absorbed by water vapor at even the best ground-based sites. FLITECAM employs large cryogenic optics and an ALADDIN III 1024 x 1024 InSb detector to inscribe an 8 arcminute field of view with 0.48 arcsec/pixel spatial resolution. The optical components are cooled with liquid nitrogen and a liquid helium reservoir is used to establish an operational temperature of 30 K for the InSb array. FLITECAM has two primary observing modes, imaging and spectroscopy. A pupil-viewing mode, for examination of the primary mirror surface, and a high-speed snapshot mode for occultation observations are also provided. Ground-based commissioning of the instrument using the Shane 3-meter telescope at UCO/Lick Observatory has been completed successfully. In addition to broad-band filters, the imaging mode accommodates several narrow-band filters. A data reduction pipeline processes dithered image sets in real-time during the flight. The grism spectroscopy mode employs three direct-ruled KRS-5 grisms and fixed slits of either 1″ x 60″ or 2″ x 60″ to yield resolving powers (FWHM) of R~1700 and 900 respectively. Observations are scripted using AORs (Astronomical Observation Requests) in both modes. A pilot survey of 3.3 micron emission in planetary nebulae performed with FLITECAM at UCO/Lick Observatory demonstrates the potential of the grism mode.

Keywords: airborne astronomy, instrumentation, grisms, PAH features

1. INTRODUCTION

One of the initial requirements for the Stratospheric Observatory for Infrared Astronomy (SOFIA) was a simple near-infrared (1-5 μm) test camera to assist with commissioning of the telescope and observatory. A field of view (FOV) of 4′ x 4′ (~5.7′ diameter) was considered sufficient, and cost considerations limited the detector to a format of 512 x 512 pixels.[1] However, at the preliminary design review there was strong encouragement to increase the field of view and convert this camera to a facility-class instrument[2,3] and to ensure that it could be co-mounted with the CCD-based High-speed Imaging Photometer for Occultations (HIPO)[4]. Although very difficult to accommodate in the space-envelope available, these requirements have been meet. FLITECAM has been constructed successfully and commissioned in ground-based observations at the UCO/ Lick Observatory (Mt. Hamilton, CA).[5,6] Developed at UCLA by a team led by Ian McLean, FLITECAM is designed to capitalize on the low background and low water vapor conditions provided by SOFIA. The completed instrument has an ~8′ diameter circular FOV inscribed within a 1024 x 1024 InSb Aladdin III detector, and provides two primary observing modes, direct imaging and grism spectroscopy, as well as a special rapid-exposure snapshot mode for occultation studies and a diagnostic pupil-viewing mode for L-band.

By designing the cryogenic part of FLITECAM to operate in a horizontal orientation at the Nasmyth focus of SOFIA (2.5 m, f/19.7) and in a vertical orientation at the Cassegrain focus of the UCO/Lick Observatory's Shane telescope (3.0 m, f/17), the instrument could be tested and evaluated independently of the SOFIA platform. The only exception is the very longest wavelengths where ground-based backgrounds are too high for broad-band imaging work. FLITECAM has been deployed to Lick Observatory for a total of eight observing runs, four of which were dedicated to commissioning of the imaging mode and the other four to the grism spectroscopy mode. Observations made during these runs have resulted in three scientific papers[7,8,9], several conference papers and two successful Ph.D. theses (Amanda K. Mainzer and Erin C. Smith).

*erincds@astro.ucla.edu

Ground-based and Airborne Instrumentation for Astronomy II, edited by Ian S. McLean, Mark M. Casali,
Proc. of SPIE Vol. 7014, 701411, (2008) · 0277-786X/08/$18 · doi: 10.1117/12.788693

The high-speed occultation mode was commissioned on the 72-inch Perkins telescope at Lowell Observatory (Flagstaff, AZ), where FLITECAM was co-mounted with HIPO (PI Edward Dunham). Here, we present a brief overview of FLITECAM and its capabilities, and the results of ground-based commissioning. We also discuss the estimated performance of FLITECAM when it is deployed on SOFIA.

2. OVERVIEW OF THE DESIGN

The optical design meets the basic requirements of FLITECAM's two primary scientific observing modes: a wide-field imaging mode with a suite of narrow and broad band filters, and a grism spectroscopy mode with sufficient resolution (R~2000; 2 pixels) to measure the strength of near-infrared water-vapor bands. Pixels subtend 0.476″ on SOFIA and image quality is very good over the inner 5.7′ diameter field where it will be limited by turbulence; images at the edge of the full 8′ field will be limited in part by residual coma. To implement the spectroscopic mode a set of three direct-ruled KRS-5 grisms are used, together with a suite of custom order-sorting filters and a pair of fixed slits in a deployable focal plane mask. A third scientific mode, which is a special case of the imaging configuration, allows rapid acquisition of frames or sub-frames for occultation studies. Another special case of the imaging configuration is the pupil-viewing mode, in which additional lenses are moved into the beam to re-image the entrance pupil onto the detector. This mode is designed to work only in the 3-4 μm band in order to evaluate the emissivity of SOFIA's primary mirror.

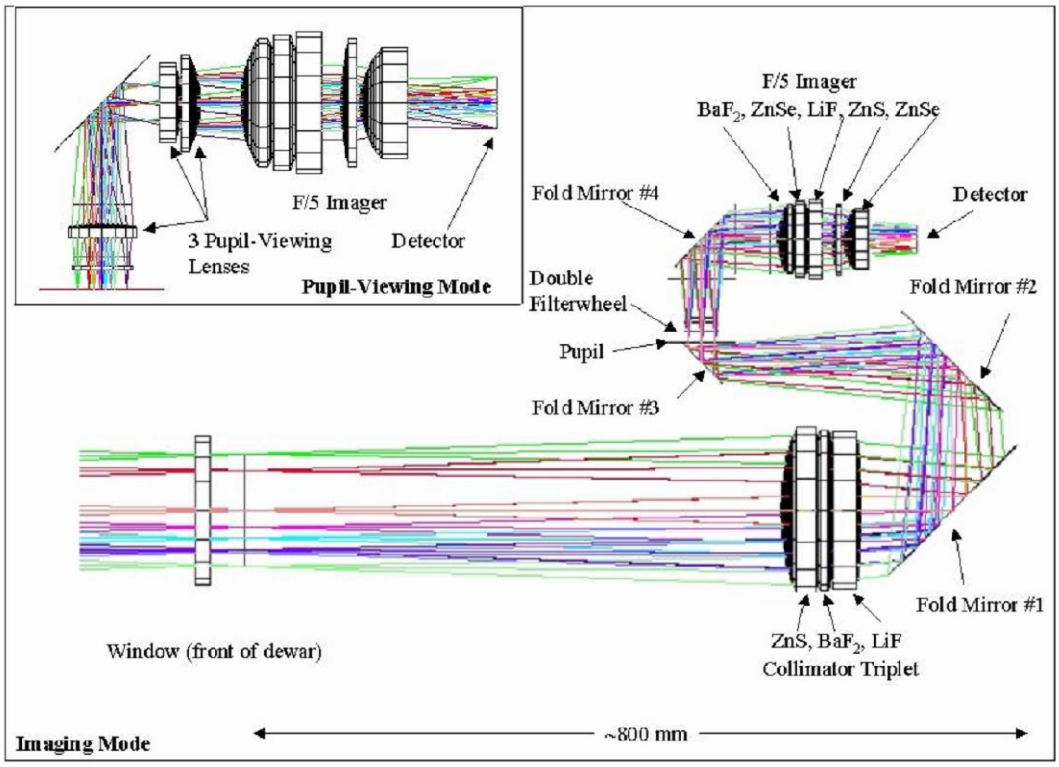

Fig. 1. The FLITECAM optical path.

Figure 1 shows the FLITECAM optical path. The telescope focus is formed just inside the entrance window (CaF_2) for both the Lick and SOFIA telescopes. As the clear aperture at the window is 140 mm, special precautions are employed to provide a dry air flow across the window for ground-based use, while on board SOFIA the cavity in front of the window can be sealed and evacuated for take-off and landing. The vacuum window is 21.5 mm thick to ensure negligible distortion due to the pressure differential. Light is then collimated and folded through a dual filter wheel, then folded back through an "F/5" camera assembly (actually f/4.675) onto the InSb detector. Given the focal ratio of the

telescope (f/19.656), the focal reduction is 4.20 and the scale is 0.476 arcsec per pixel (27 μm). In its collimator section, FLITECAM employs three large (~165 mm diameter) lenses to inscribe the entire SOFIA pupil on a 1024 x 1024 InSb Aladdin III detector. To facilitate co-mounting with HIPO the entrance window is offset from the center line of the cylindrical cryostat. In addition, to keep the overall length of the optical chamber as small as possible the beam is folded with four mirrors. The InSb detector is controlled by a custom set of electronics made by Mauna Kea Infrared (MKIR, HI). Electronics mounted on the cryostat read out the detector, amplify and convert the signals to digital packets, and transmit them via fiber optic cable to the MKIR computer located in a remote rack called the "PI" rack. FITS headers are populated by the MKIR computer. Astronomers can adjust the exposure time and the read mode of the detector through the astronomer's graphical user interface on the host computer in the PI rack. The fastest exposure time for the full 1024 x 1024 array is 0.3 seconds. A sub-array of 512 x 512 pixels can be read out in 0.1 seconds and a 64 x 64 sub-array allows 0.02 s exposures (50 Hz frame rate). FLITECAM can also operate in a "movie mode" when co-mounted with the HIPO instrument. This mode allows rapid acquisition of multiple frames with minimum dead-time for use in occultation studies.

To obtain the pupil-viewing mode (shown in insert at upper left of Figure 1) three additional lenses are introduced into the beam, one is located in the second filter wheel and the other two are co-mounted on a slide. Crystal fluorides are used in several places in the optical design. These lenses are very sensitive to thermal shock. Consequently, the instrument is cooled-down very slowly over a 2-day interval using a strict procedure for cryogen filling and internal temperature changes are monitored with a set of eight temperature probes.

FLITECAM utilizes four cryogenic mechanisms: an aperture slide, which moves the slit mask in and out of the beam for spectroscopy, two independent filter wheels, and another slide which carries the pupil-viewing doublet in and out of the beam immediately in front of the F/5 camera. Stepper motors prepared for cryogenic operation inside the instrument are used together with a series of microswitches for positioning each of these mechanisms. A graphical user interface provides easy control and display of the state of each mechanism. Motor controllers, temperature control and monitoring devices, power supplies, and multiplexers are packaged in a rack mounted on the telescope and located close to the cryostat (~ 3 m); this rack is known as the "counterweight" or CW rack. A panel of colored indicator lights on the CW rack motor control box also indicates microswitch status. All four mechanisms have been tested successfully in both the lab environment and at Lick observatory.

One unique consideration for FLITECAM, and all instruments developed for SOFIA, is referred to as "airworthiness" which covers all aspects of safety, especially for in-flight operations. FLITECAM is designed to operate inside the pressurized cabin of a modified commercial Boeing 747 jet plane flying at up to 45,000 feet. Stringent safety requirements are imposed. All fabricated components, fasteners and cables are made of certified materials. Likewise, safety documentation and handling procedures are required for every aspect and every possible failure condition of the instrument in order to ensure personnel safety and safe operation of the aircraft at all times. The FLITECAM instrument consists of three major components, the instrument cryostat and mounting flange, the PI rack, and the counterweight (CW) rack. Figure 2 shows the three components deployed in the laboratory. All three components conform to both NASA and Federal Aviation Authority (FAA) airworthiness requirements.

The PI rack houses three computers used in the operation of FLITECAM: they are named Farscape, Stargate and MKIR. Farscape and Stargate are PCs running Windows NT, while MKIR is a custom-made Solaris box. Stargate controls the astronomer's interface, while Farscape is the main data reduction computer and MKIR controls and reads out the detector. The PI rack also includes two sets of keyboard trays and monitors that can be completely folded and stowed for takeoff and landing. A serial to fiber optic mux communicates with an identical mux located on the CW rack. The racks are provided by the SOFIA project and are already FAA-certified. No alterations to the racks can be made.

User interaction with FLITECAM is accomplished through the astronomer's graphical user interface (GUI) on the Stargate computer, located in the PI rack. This GUI allows the user to change the state of a mechanism state, select the sub-array size on the detector and monitor temperatures and liquid helium levels. Another window allows interactive positioning of targets on the FLITECAM array, which is especially useful in placing selected targets on the spectroscopy slit. A separate screen is used to access the Quick-look software and monitor data reduction (see Figure 2).

The CW rack houses all the mechanism power supplies and monitoring equipment needed to operate FLITECAM. From top to bottom the components in this rack are: a Pulizzi power controller; a liquid helium level monitor; a Lakeshore 218 for monitoring temperatures inside the cryostat; a Lakeshore 330 for control of the FLITECAM detector; the detector power supply; and the motor box, which powers the four internal mechanisms and monitors the internal microswitches.

Six serial cables connect the CW rack to the instrument cryostat. Because alteration of this rack would result in loss of airworthiness certification, use of this rack at Lick Observatory required the construction of a 'cradle' for protection. The cradle can be seen in Figure 2 as the green Unistrut surrounding the gold-hued rack. All bolt holes were made in the Unistrut cradle, rather than the CW rack itself when the instrument was deployed at Lick Observatory.

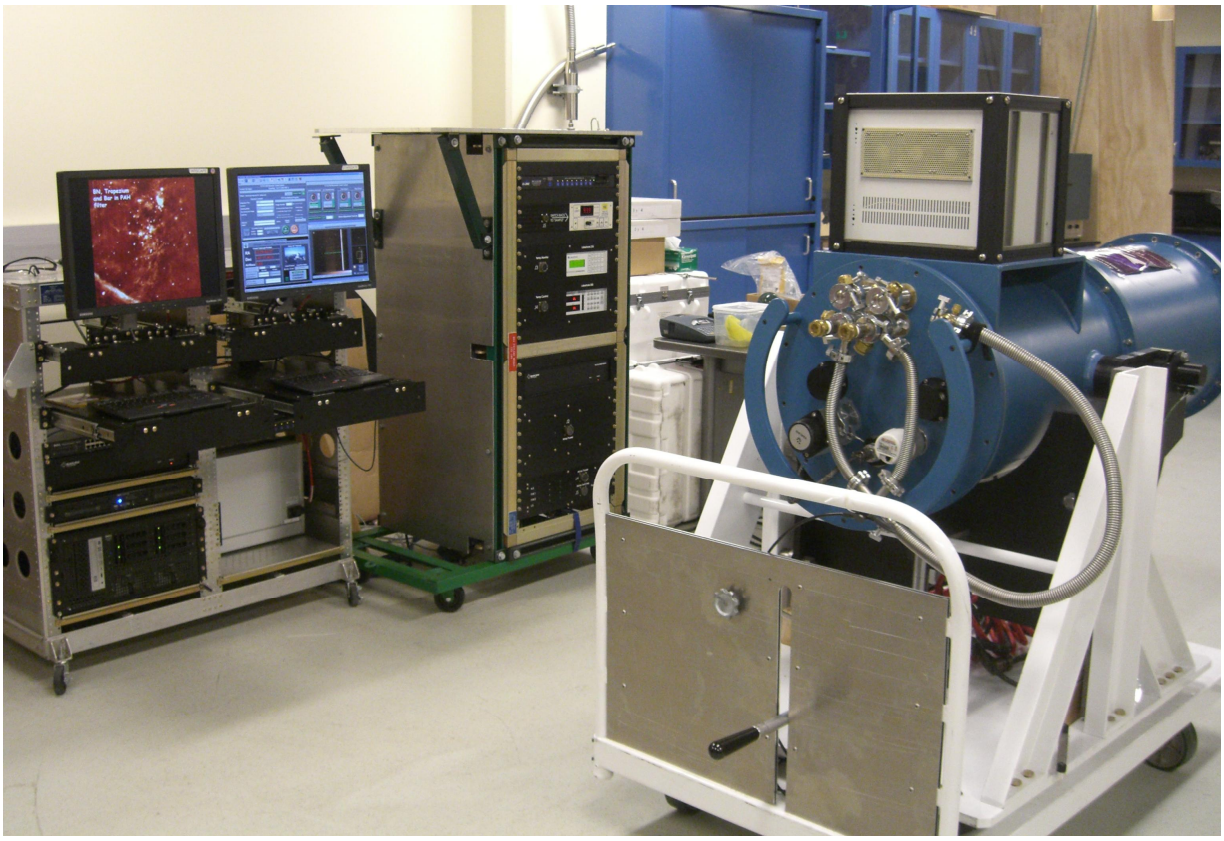

Fig. 2. FLITECAM in the IR Lab at UCLA. In the background from left to right are the PI rack with dual computer screens and the CW rack (vertical). In the foreground is the cryostat (blue) mounted on its handling frame (white).

The FLITECAM cryostat is a thick-walled cylinder about 1.52 m (5 ft) long and 0.49 m (1.6 ft) in diameter, with a box of electronics mounted on the top rear section. The instrument is operated under vacuum and cooled to ~90 K in order to reduce the background incident on the detector. The front half of the cryostat houses the opto-mechanical system and the InSb detector, while the back section holds two 20 liter liquid cryogen containers, one for liquid nitrogen and the other for liquid helium. FLITECAM uses liquid cryogens instead of the more common closed cycle refrigerators (CCRs) because of airworthiness requirements. The back end of the cryostat (shown in Figure 2) has a system of non-return valves for the safe venting of cryogen boil-off gases during operation. Both the nitrogen and helium vent systems also have additional burst disks (2 for nitrogen, 5 for helium) which can quickly release internal pressure in the case of rapid boil-off in an emergency situation (e.g., sudden loss of cryostat vacuum).

3. SOFTWARE

3.1 Astronomical Observation Requests (AORs)

Observations with FLITECAM can be made in two ways. Manually, by setting the exposure time and moving individual mechanisms to the correct initial state for the desired observation, or through automated scripts called Astronomical Observation Requests (AORs). AORs are selected from the Astronomer's GUI on the Stargate computer. FLITECAM can execute two kinds of AORs, either spectroscopy or imaging. Spectroscopy AORs will move the aperture slide to

bring the spectroscopic slit into the beam, and will move the filter wheels to give the selected grism/order sorting filter combination. The AOR will then execute either an AB or ABBA nod pattern, where A and B refer to the position of the object on the slit. The default nod size is 26 arc seconds. For extended objects off-slit nodding is also available. For imaging mode the AOR has a library of scalable "dither" patterns including regular grids (box-5, box-9) and several 9-point dither patterns with randomized spatial frequencies. An adjustable scale factor allows selection of dither pattern size. Any imaging filter can be selected for a dither AOR. Once pattern and filter selections have been made, the AOR generates an estimated timeline for completion of the observations including the necessary mechanism moves. The AOR timeline calculation takes into account the pre-AOR state of the instrument—no unnecessary mechanism moves are included in the execution of an AOR. When executed, the AOR will complete all mechanism moves, all exposures and all telescope nods automatically. AORs are the primary method for obtaining scientific data with FLITECAM, both on the ground and aboard SOFIA. Airborne AORs will also include guide star selection and acquisition, which will further streamline the observing process.

3.1 Data Reduction Pipeline (DRP)

Imaging AORs can be auto-reduced using the Data Reduction Pipeline (DRP) developed by Ralph Shuping (USRA SOFIA Project). The DRP is an IDL package that creates flat-fielded, fully-reduced fits images from a set of dithered images. Auto-reduction of dithered sets of images runs automatically whenever a set completes. If the field is too crowded for extraction of a sky-flat then a separate flat-field frame can be designated. Only the region fully within the inscribed square field of view of the detector (5.6′ x 5.6′) is used by the DRP. The DRP itself runs on Farscape, the main data-reduction computer.

4. GROUND-BASED COMMISSIONING

4.1 Lick Observatory

Because the focal length of the 2.5 m, f/19.7 SOFIA telescope is well matched with the 3 m, f/17 Shane telescope at Lick Observatory, FLITECAM can be mounted to the Shane telescope without use of additional optics. The plate scales are 0.43 arcsec/pixel and 0.48 arcsec/ pixel at Lick and SOFIA, respectively. Typically, seeing at Lick ranges from 1″ to 1.5″, which is somewhat better than the expected near-infrared image quality with SOFIA (~1″ to 3.5″ depending on wavelength). FLITECAM was successfully used at Lick Observatory in October of 2003. By October 2006 the final deliverable system, complete with certified racks was commissioned, with all required modes functional and tested. As mentioned, scientific results from these runs have been published[7,8,9].

4.2 Pupil viewing mode

One of FLITECAM's diagnostic functions is evaluation of the SOFIA primary mirror from time to time. To view the primary (and secondary) mirrors the optical prescription of FLITECAM must be changed to image the entrance pupil onto the FLITECAM detector. We are most interested in characterizing the emissivity in the thermal infrared beyond 3 microns. To keep the pupil-viewing system as simple as possible it was designed for the L-band only. Imaging the full pupil of FLITECAM requires two sets of optics: a singlet lens mounted in the second FLITECAM filter wheel and a doublet lens located in front of the camera optics. The required lenses are listed in Table 1. Currently, FLITECAM has a Lyot stop located at the pupil which falls near the entrance to the filter wheel module. The Lyot stop consists of a disk to match the SOFIA secondary mirror and three support wires aligned with the secondary support vanes. In pupil-viewing mode the image of the Lyot stop should be in focus on the detector at 3.5 μm.

Table 1: Pupil-Viewing lenses.

Lens Name	Location	Lens Material	Diameter (inches)	Width (inches)	R1 (inches)	R2 (inches)
L1	FW2	Silicon	1.494	0.59	3.779	6.230
L2	PV slide	BaF2	1.73	0.368	-1.102	3.423
L3	PV slide	Silicon	2.123	0.162	-3.307	2.352

While L1 is carried by the second filter wheel, a special slide mechanism is dedicated to moving the doublet, comprised of L2 and L3, in and out of the beam. The mechanism is a simple, direct-drive rack and pinion system driving a linear slide prepared for vacuum-cryogenic operation. Attached to the top of the slide are three detents. These detents actuate micro-switches mounted to the front face of the bulkhead, and also retain the slide in place when positioned in or out of the beam. The PV slide is controlled in the same way as the other mechanisms in the FLITECAM instrument.

Because it was designed only for use at L-band, the pupil-viewing mode was difficult to test under the correct conditions due to the high thermal backgrounds at Lick Observatory where the telescope is much warmer than SOFIA will be. Attempts to image the full field in our narrowest band at 3.6 μm led to saturation; sub-arrays in this case are not helpful because we must image the entire pupil. By inserting the cold slit mask in the focal plane all of the thermal background is eliminated and it became possible to image the cold Lyot stop directly, as shown on the left side of Figure 3. The central obscuration is clear and in focus, as are the 3 spider-leg support structures. This image shows the PV mode to be operational and in focus at the required wavelength. Because the optical design is not achromatic pupil images become defocused away from 3.6 μm, especially at shorter wavelengths. Nevertheless, even a poorly focused pupil image at 2.2 μm, where the background is much smaller, is useful to show the degree of alignment between the instrument and the telescope. The right hand image in Figure 3 was obtained at Lick Observatory with FLITECAM in pupil-viewing mode by using K-band. The Lyot stop and the large secondary mirror of the Shane telescope, with its 4-point mounting, are out of focus, but it can be seen that a small centering error exists. From the known geometry the tilt can be determined and a small shim used to correct the alignment. Aboard SOFIA the background will be sufficiently low to allow L-band imaging of the fully illuminated pupil.

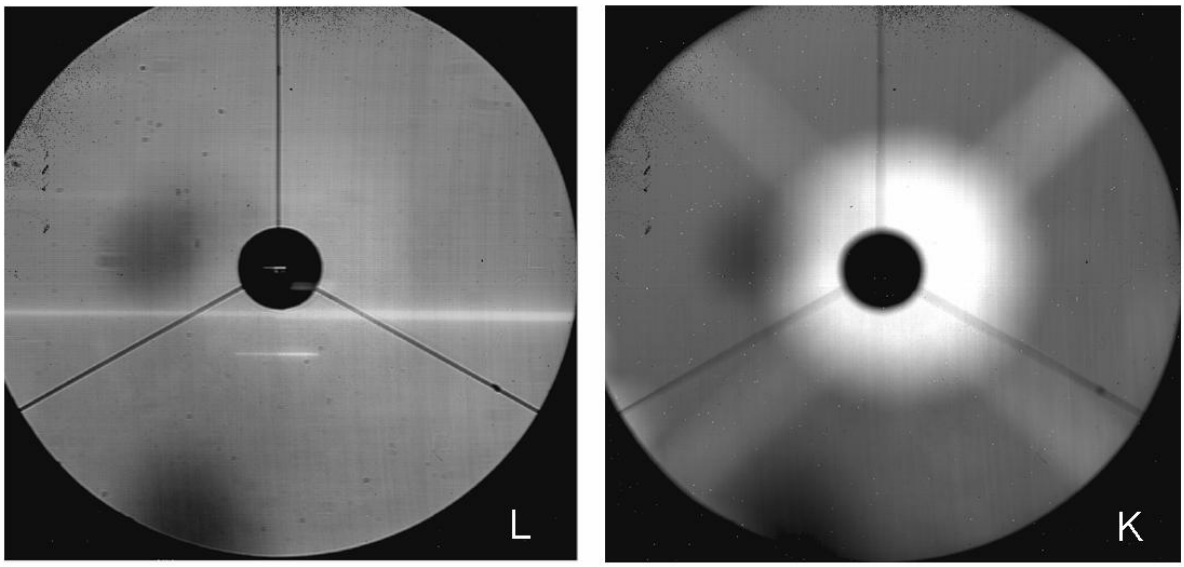

Fig. 3. Left: a FLITECAM pupil image at 3.6 μm with the cold slit mask in place to reduce thermal background illustrates good focus. Right: an image of the secondary mirror of the Shane 3-m telescope at 2.2 μm, where the pupil-viewing system provides poorly focused images but the full field can be obtained because the background is much less.

4.3 Narrow band imaging

One advantage FLITECAM has over current space-borne near-infrared instruments is the ability to perform narrow band imaging in the 2-5 μm regime. With SOFIA, FLITECAM will be able to image features totally or partially absorbed by telluric water vapor. Additionally, the lower background due to the cold telescope (240 K) and cold, thin atmosphere will allow imaging of low surface brightness features. One important spectral feature in the 2-5 μm regime is the 3.3 μm emission from polycyclic aromatic hydrocarbons (PAHs). This broad feature is bright enough in some targets to allow background-limited narrow-band imaging. We imaged several targets, including star formation regions and planetary nebulae with a 1% wide filter centered at 3.29 μm, and with a slightly broader filter centered at 3.6 μm for continuum comparison. Images were taken with a 512 x 512 sub-array, and an on-chip integration time of 0.2 second. Multiple

frames were co-added. All targets were observed using a box-9 dither pattern and were auto-reduced with the FLITECAM DRP.

Figure 4 shows the result for observations of NGC 7027, a young, high-excitation planetary nebula. The most obvious difference between the continuum and PAH emission is that the latter exhibits a more 'box-like' distribution than the continuum emission. This conclusion is borne out by higher spatial resolution imaging and spectroscopy. As shown by the insert of a 3-micron spectrum, the identification of PAH emission is confirmed by FLITECAM grism spectroscopy.

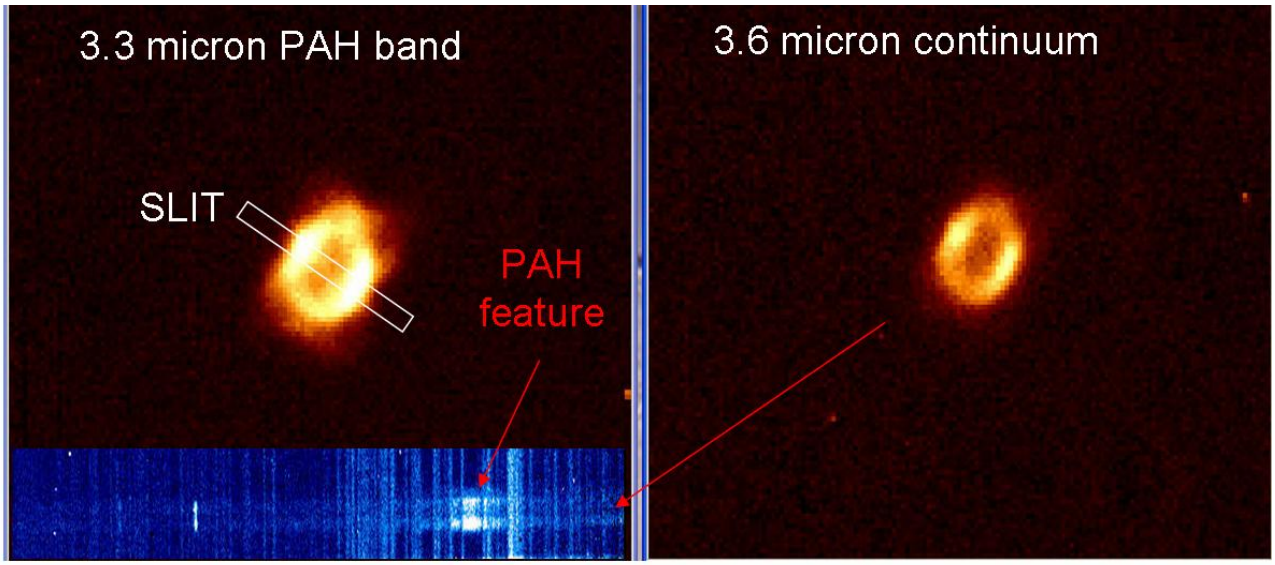

Fig. 4. Narrow band images of the young planetary nebula NGC7027 on and off the 3.3μm PAH emission feature. The insert on the lower left is a 3-micron region spectrum obtained with the slit oriented as shown.

4.4 Spectroscopy mode

Initially, the requirement for FLITECAM to help calibrate SOFIA's on-board water vapor monitor by spectroscopic observations of telluric water lines at 2.5 μm drove the need for a grism spectroscopy mode. With minor changes however, this requirement was expanded to provide FLITECAM with a more general spectroscopic capability giving wavelength coverage over nearly the entire 1 to 5 μm regime. Grisms offer a relatively inexpensive and simple method of adding spectroscopic capability to a camera without altering the camera's optical path. There are three components to any grism spectroscopy system: an entrance slit, an order sorting filter and a grism. A grism is usually formed by a prism of high index of refraction with a transmission grating either adhered to (resin grism) or etched into (direct-ruled grism) one face.

FLITECAM uses direct-ruled grisms because the adhesive used in resin grisms exhibits absorption features in the near-infrared at the same wavelengths where PAH emission is typically observed[10]. Grisms exploit Snell's law by using refraction by the prism material to bend the light diffracted by the grating back onto the 'normal' optical path. Figure 5 shows the basic geometry of a grism.

Assuming right-angled prism geometry, the basic grism equation is given by[11]

$$T\, m\, \lambda_c = (n - 1)\, \sin A$$

Where T is the groove spacing, m is the order number and A is the prism angle. By changing the groove spacing, T, we can select the central wavelength λ_c.

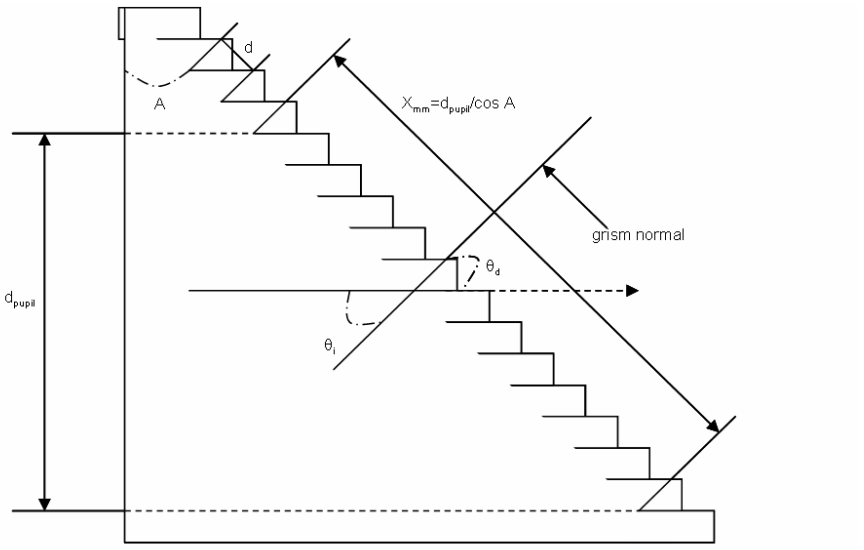

Fig. 5. Illustration of basic grism geometry

The use of a grating for dispersion results in multiple orders of diffraction and overlapping spectra on the detector. Order selection is accomplished by filtering the light with an order sorting filter (OSF). Each of FLITECAM's grisms (labeled A, B and C) can be used in 3 orders, resulting in 9 bands of coverage.

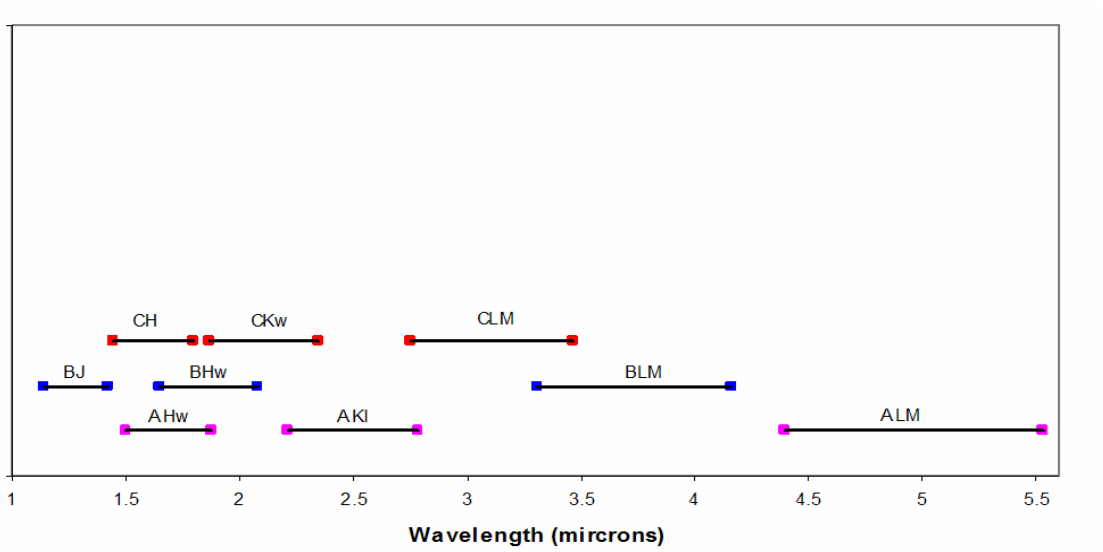

Fig. 6. Wavelength coverage of the FLITECAM grism spectroscopy mode. The first letter in each band's name refers to the KRS-5 grism used. The last letter(s) call out the order sorting filter.

Figure 6 shows the grism band coverage for FLITECAM, with each grism/OSF combination labeled. Table 2 lists the spectroscopic bands in terms of initial and final wavelength, along with central wavelength, order and order sorting filter. The entrance slit is a 120″ long rectangular slot cut in an aluminum plate; half the length is 1″ wide and the other half is 2″ wide. The slit is slightly offset from the center of the field to ensure that the spectrum only crosses one boundary of the four-quadrant InSb array. The slit-mask plate is attached to a computer-controlled slide mechanism. Motion of the plate is controlled from the astronomer's GUI on the Stargate computer. Figure 7 shows the grisms as installed in the FLITECAM filter wheel. A more detailed account of grism selection and the development of the spectroscopy mode is given by Smith & McLean (2006)[12].

Table 2. Grism specifications

Grism	T (l/mm)	Order	OSF	λi	λc	λf
A	162.75	1	L&M	4.395	4.96	5.533
A	162.75	2	Klong	2.216	2.5	2.784
A	162.75	3	Hwide	1.497	1.69	1.877
B	217	1	L&M	3.307	3.73	4.16
B	217	2	Hwide	1.649	1.86	2.076
B	217	3	J	1.14	1.28	1.424
C	130.2	2	L&M	2.756	3.11	3.467
C	130.2	3	Kwide	1.872	2.11	2.346
C	130.2	4	Hwide	1.445	1.62	1.801

Grism spectroscopy mode was first tested in March 2004, and was commissioned at Lick Observatory in October 2004. Figure 8 shows the raw output from the grism spectroscopy mode for an A0V star, Leo 69. We have commissioned all but the longest wavelength grism band (ALM) at the telescope. The A/LM grism band extends to beyond 5 μm, and thus saturates even with the shortest exposure time. This band will be commissioned aboard SOFIA, where the backgrounds are expected to be lower by more than a factor of 10.

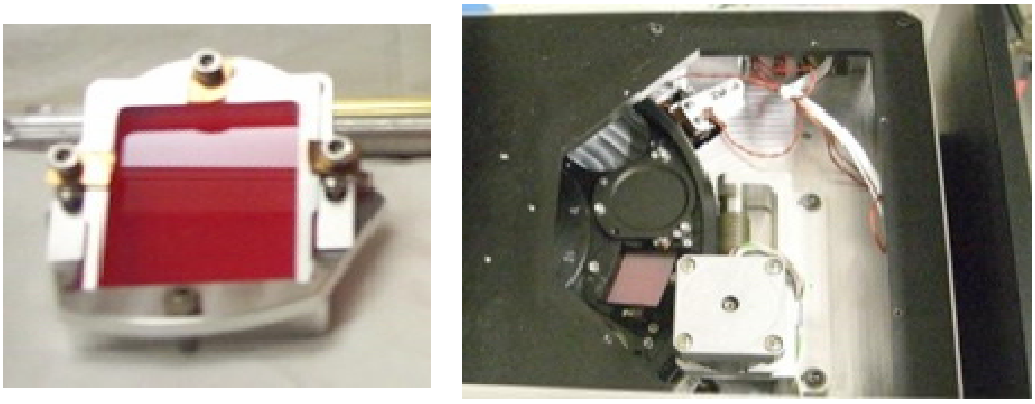

Fig. 7. Left: KRS-5 grism installed in its holder. Right: The grism installed in the FLITECAM filter wheel.

Fig. 8. The spectrum of 69 Leo (A0V) from 1.872-2.346 μm: the spectral trace of the star can be seen in the upper half of the image, corresponding to the narrower (1″) slit. Numerous OH lines delineate both slit sections of the mask.

FLITECAM's grism spectroscopy mode was used in a scientific survey of PAH emission in planetary nebulae. Polycyclic aromatic hydrocarbons (PAHs) are small, benzene-like molecules believed to form in the outflows of evolved, carbon rich, intermediate mass stars. When excited by UV photons, these molecules emit broad bands throughout the near and mid-infrared wavelength regime, most notably at 3.3, 6.2, 7.7 8.6 and 11.2 microns[13,14]. PAH emission has been observed in a variety of objects, including planetary nebulae, star forming regions and, most recently in external galaxies. The ubiquity of PAH emission has made it an important topic for astronomical research, but the wavelengths of the features make ground-based studies very difficult. As a precursor to observations with SOFIA, we used the UCO/Lick Observatory 3-m telescope to observe a sample of planetary nebulae (PN) and pre-planetary nebulae (pPN) at 3.3 μm with the FLITECAM grism spectroscopy mode.

The fully reduced spectrum of the young, high excitation planetary nebula NGC 7027 is shown in Figure 9. Broad PAH emission is clearly evident at 3.29 μm, as is the narrow Pfund-δ hydrogen emission feature superimposed on the PAH band. Also evident is the telluric contribution, which appears as excess noise on the blue edge of the PAH band and as missing data due to a saturated H_2O feature on the red side. Because the atmosphere at Lick Observatory is highly variable in water vapor content, we used the atmospheric modeling program, ATRAN developed by Steve Lord[15], for telluric correction instead of a standard star. Of the 20 objects (PN, pPNs and AGB stars) observed in this pilot study, 11 showed PAH emission at 3.3 μm. The results of this survey are published in Smith & McLean (2008)[9].

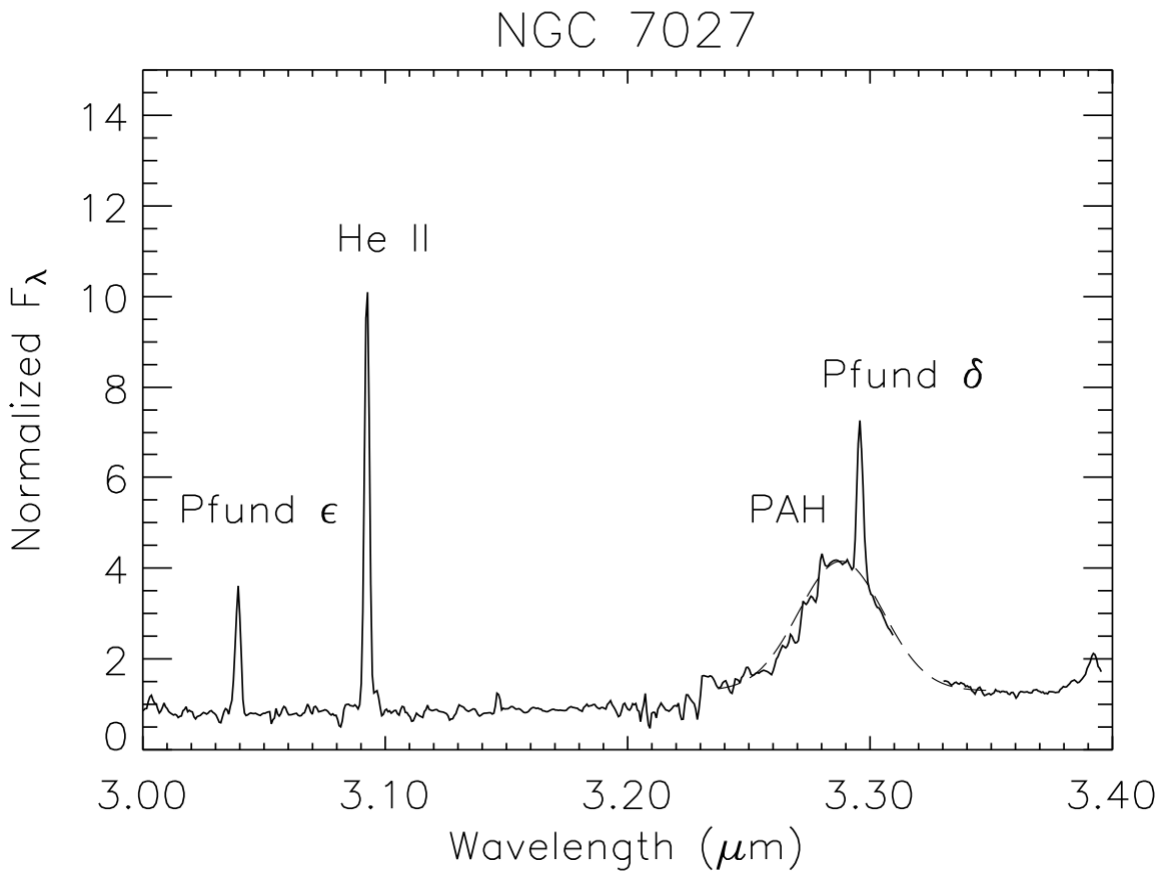

Fig. 9. Reduced 3 micron spectrum of NGC 7027, a young, high excitation planetary nebula. Strong emission from ionized helium and hydrogen is clearly visible together with the broad PAH feature centered at 3.29 microns. The dashed line over-plotted on the PAH emission feature is the best-fitting Gaussian from which an equivalent width is derived.

5. AIRBORNE SENSITIVITY OF FLITECAM

FLITECAM's true scientific potential lies with SOFIA. Reduced water vapor levels and a lower thermal background compared to even the best ground-based observatories will make FLITECAM 10-20 times more sensitive in certain parts of the 2-5 micron region. In addition, backgrounds will vary on a much longer timescale than for ground-based observing in this regime, allowing more stable conditions and much longer exposures.

Figure 10 shows the estimated broad-band, point-source sensitivity for FLITECAM on SOFIA, assuming a telescope with a temperature of 240 K and 15% emissivity, and assuming a seeing profile with a FWHM ranging from 3.5″ to 1.5″ over the wavelength interval 1-5 μm. Sensitivity is quoted as the flux density (in μJy) for a signal-to-noise ratio of 4 in 900 s (on source) integration time; figures in brackets are the equivalent magnitudes on the Vega system. In spectroscopy mode, the CLM and BLM bands will be capable of much longer integration times, enabling fainter objects to be reached, and the ALM band becomes open for the first time.

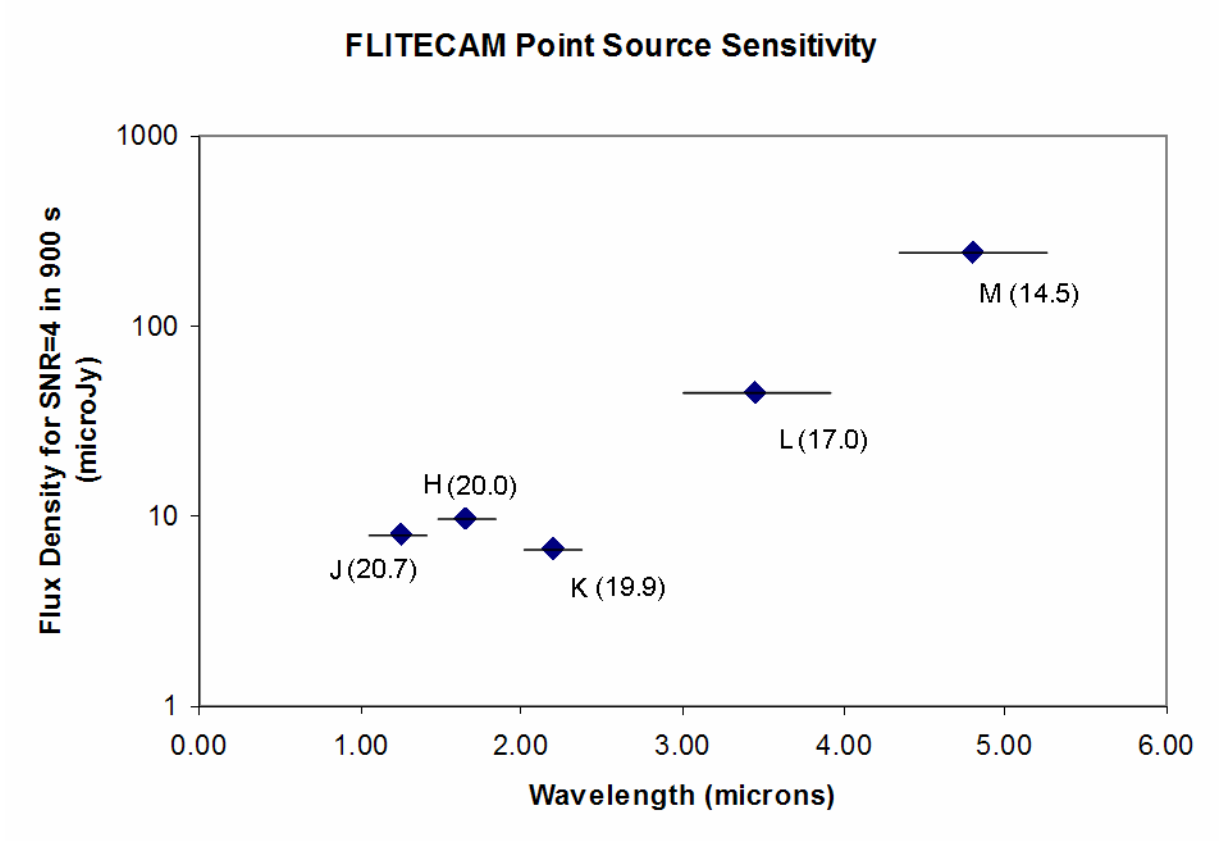

Fig. 10. Predicted broad-band sensitivity for FLITECAM for point source detection (S/N=4 in 900 s) aboard SOFIA.

ACKNOWLEDGEMENTS

The successful commissioning of the FLITECAM instrument would not have been possible without the hard work of the entire FLITECAM project team, past and present, including Ted Aliado, George Brims, John Canfield, Don Figer, John Goulter, Jochen Horn, Evan Kress, Ken Magnone, Nick Magnone, Amy Mainzer, John Milburn, Andrew Oldag, Mike Spencer, Gunnar Skulason, and Tatyana Silvers. Special thanks also to John Rayner for his help with the KRS-5 grisms. FLITECAM is primarily funded by a grant from USRA with partially support from UCO and UCLA. Erin Smith is supported by a NASA Graduate Student Research Fellowship (GSRP).

REFERENCES

[1] Figer, D. F.; McLean I. S. and Becklin, E. E., "FLITECAM: a 1-5 micron camera for testing the performance of SOFIA," in *Infrared Astronomical Instrumentation*, A. Fowler, ed., Proc. SPIE 3354, 1179-1184 (1998).

[2] Horn, J. M. M. and McLean, I. S., "The optical design of FLITECAM," Proc. SPIE 4008, 979-989 (2000).

[3] Horn, J. M. M.; Becklin, E. E.; Bendiksen, O.; Brims, G.; Goulter, J.; Kress, E.; Magnone, N.; McLean, I. S.; Milburn, J.; Molayem, N.; Moseley, H. S.; and Spencer, M., "FLITECAM: A near-infrared camera for test and science applications on SOFIA," Proc. SPIE 4014, 65-76 (2000).

[4] Dunham, E. W.; Elliot, J. L.; Bida, T. A. and Taylor, B. W., "HIPO-a high-speed imaging photometer for occultations," Proc. SPIE 5492, 592-603 (2004).

[5] Mainzer, A. K.; McLean, I. S.; Aliado, T.; Becklin, E. E.; Brims, G.; Goulter, J.; Kress, E.; Magnone, N.; Milburn, J.; Skulason, G.; and Spencer, M., "Characterization of FLITECAM: the first light camera for SOFIA," Proc. SPIE 4857, 21-28 (2003).

[6] McLean, I. S.; Smith, E. C.; Aliado, T.; Brims, G.; Kress, E.; Magnone, K.; Milburn, J.; Oldag, A.; Silvers, T.; and Skulason, G., "FLITECAM, a 1-5 micron camera and spectrometer for SOFIA, " Proc. SPIE*,* 6269, 168-179 (2006).

[7] Mainzer, A. K. and McLean, I. S., "Using narrowband photometry to detect young brown dwarfs in IC 348," *Astrophys. J.*, 597, 555-565 (2003).

[8] Mainzer, A. K.; McLean, I. S.; Sievers, J. L. and Young E. T., "Using narrowband photometry to classify stars and brown dwarfs," *Astrophys. J.*, 604, 832-841(2004).

[9] Smith, E. C. D. and McLean, I. S., "A survey of 3.3 micron PAH emission in Planetary Nebulae", *Astrophys. J.*, 676, 408-415 (2008).

[10] Rayner, J. T., "Evaluation of a solid KRS-5 Grism for Infrared Astronomoy," in *Infrared Astronomical Instrumentation*, A. Fowler, ed., Proc. SPIE 3354, 289-294 (1998).

[11] McLean, I. S., *Electronic Imaging in Astronomy*, Wiley-Praxis, Chichester, UK, 76-80 (1997).

[12] Smith, E. C. and McLean, I. S., "Grism spectroscopy with FLITECAM," Proc. SPIE, 6269, 50-57 (2006).

[13] Allamandola, L. J., Tielens, G. G. M., and Barker, J. R., "Interstellar polycyclic aromatic hydrocarbons: the infrared emission bands, the excitation/emission mechanism, and the astrophysical implications," *Astrophys. J. S.*, 71, 733-775 (1989).

[14] Roche, P. F., Lucas, P. W., Hoare, M. G., Aitken, D. K., and Smith, C. H., "An investigation of the 3 micron emission bands in planetary nebulae," *MNRAS*, 280, 924-936 (1996).

[15] Lord, S. D., "A new software tool for computing Earth's atmospheric transmission of near- and far infrared radiation," NASA TM103957, (1992).